Spin polarization control via magnetic barriers and spin-orbit effects

Anh T. Ngo,[1] J. M. Villas-Bôas,[1,2] and Sergio E. Ulloa[1]
[1]*Department of Physics and Astronomy, and Nanoscale and Quantum Phenomena Institute, Ohio University, Athens, Ohio 45701-2979, USA*
[2]*Walter Schottky Institut, Technische Universität München, Am Coulombwall 3, D-85748 Garching, Germany*

(Received 5 June 2008; revised manuscript received 25 September 2008; published 10 December 2008)

We investigate the spin-dependent transport properties of two-dimensional electron-gas systems formed in diluted magnetic semiconductors and in the presence of Rashba spin-orbit interaction in the framework of the scattering matrix approach. We focus on nanostructures consisting of realistic magnetic barriers produced by the deposition of ferromagnetic strips on heterostructures. We calculate spin-dependent conductance of such barrier systems and show that the magnetization pattern of the strips, the tunable spin-orbit coupling, and the enhanced Zeeman splitting have strong effects on the conductance of the structure. We describe how these effects can be employed in the efficient control of spin polarization via the application of moderate fields.

DOI: 10.1103/PhysRevB.78.245310 PACS number(s): 73.23.Ad, 72.25.−b, 72.10.−d, 71.70.Ej

I. INTRODUCTION

Spin-orbit coupling in semiconductors intrinsically connects the spin of an electron to its momentum,[1] providing a pathway for electrically initializing and manipulating electron spins for applications in spintronics[2,3] and spin-based quantum information processing.[4] This coupling can be regulated with quantum confinement in semiconductor heterostructures through band-structure engineering, as well as by the application of external electric fields, as in the celebrated spin field-effect transistor proposed by Datta and Das.[5] Using diluted magnetic semiconductors (DMS) in such systems provides an additional degree of control of the transport properties. In particular, when an external magnetic field is applied, the magnetic dopant spins align, giving rise to a strong exchange field that acts on the electron spin. This *s-d* exchange interaction between the electron spin in the conduction band and the localized magnetic ions induces a giant Zeeman splitting. The effect has been recently explored theoretically as a way to enhance the transport response of two-dimensional electron-gas (2DEG) systems.[6]

In this paper we investigate the spin-dependent transport properties of 2DEG systems formed in diluted magnetic semiconductors and take into account the electric-field-dependent Rashba spin-orbit interaction (SOI). We focus our attention on nanostructures consisting of realistic magnetic barriers produced by the deposition of ferromagnetic strips near the heterostructures,[7] providing a relatively strong inhomogeneous magnetic field on the 2DEG.[8] We show how the conductance of the 2DEG depends strongly on the magnetization pattern of the strips, as well as on geometry and externally applied electric fields. We demonstrate that significant spin polarization (exceeding 50%) can be obtained at low temperatures for ferromagnetic strips of typical dimensions and magnetization. We should note that other theoretical work has explored the spin polarization introduced by magnetic modulation in different systems,[9,10] and especially the role of spin orbit in two-dimensional systems.[11] We demonstrate here that the implementation of magnetic barriers in DMS electron systems results in enhanced and well-controlled spin polarization even for shorter barriers, thanks to the enhanced Zeeman effect in these structures.

II. MODEL AND THEORETICAL APPROACH

Figure 1 illustrates the type of magnetic barrier which can be created by the deposition of a ferromagnetic strip on the surface of a heterostructure. In this case the magnetization is assumed perpendicular to the 2DEG located at a distance z_0 below the surface. For this strip of width d and thickness h, the magnetic field along the $\hat{z}$ axis is given by[7]

$$B = B_0[f(x+d/2) - f(x-d/2)], \tag{1}$$

where $B_0 = M_0 h/d$, $f(x) = 2xd/(x^2+z_0^2)$, and M_0 is the magnetization of the ferromagnetic strip. The in-plane field component can be assumed negligible for this configuration.[7] We should mention that deposition of dysprosium strips results in magnetic fields estimated to be as large as 1 T in the vicinity of the 2DEG (Ref. 8); from this we take $B_0 = 0.1$ T to be a realistic value.

The Hamiltonian of the 2DEG (in the xy plane) is realized in the lowest subband of the semiconductor heterostructure with effective mass m^*, and includes the Rashba SOI due to z confinement, as well as due to applied electric fields via a gate voltage on the strip, characterized by the coupling constant α_z, the Zeeman term with electronic g factor, and the *s-d* exchange interaction

$$H = \frac{1}{2m^*}(\Pi_x^2 + \Pi_y^2) - \frac{\alpha_z}{\hbar}(\sigma_x \Pi_y - \sigma_y \Pi_x) + \frac{g\mu_B \sigma_z}{2} B(x) + j_{sd} \sum_i s(r) \cdot S(R_i)\delta(r - R_i), \tag{2}$$

where Π_μ denotes the kinetic momentum and σ_μ is the Pauli spin matrices. S is the spin of the localized $3d^5$ electrons of Mn^{2+} ions with $S = 5/2$ and s is the electron spin in the 2DEG. We assume that the magnetic ions are distributed homogeneously in the DMS, and that the extended nature of the electronic wave function spans a large number of magnetic ions, allowing the use of a molecular-field approximation to

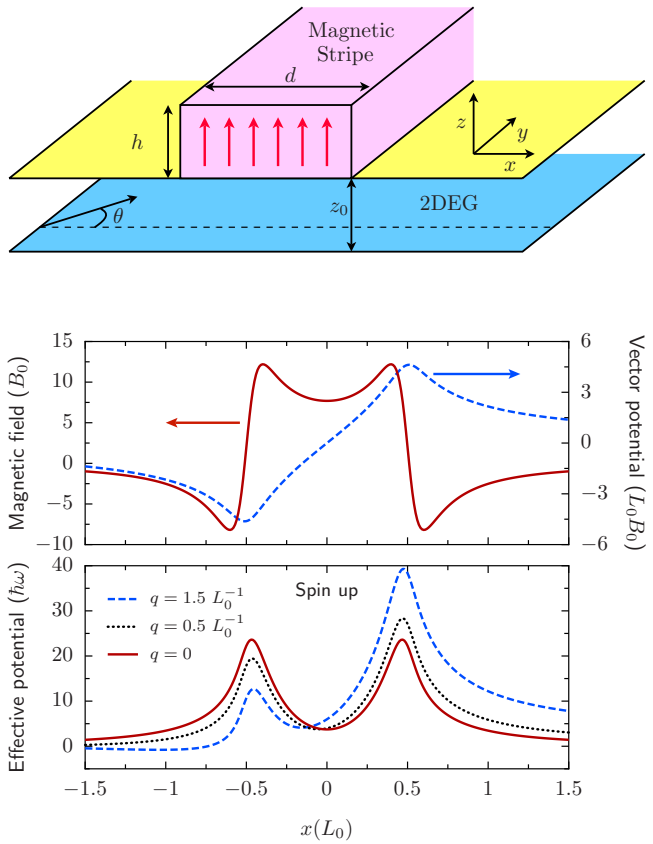

FIG. 1. (Color online) Top diagram illustrates magnetic strip with perpendicular magnetization over a 2DEG layer. The magnetization of the strip results in the magnetic barrier and vector potential shown in the middle panel. Bottom panel shows effective potential V_e for different q values [Eq. (4)]. Rashba SOI is assumed present only under the strip via an applied gate voltage. Structural parameters chosen as $d=1$ and $z_0=0.1$, in units of the magnetic length $L_0=\sqrt{\hbar/eB_0}=81$ nm for $B_0=0.1$ T.

replace the magnetic-ion spin operator S_i with the thermal and spatial average $\langle S_z\rangle$ along the external magnetic-field direction. This approach has been proven suitable in previous studies.[12,13] Correspondingly, the exchange interaction in Eq. (2) can be written as a Zeeman-type term, $J_{sd}\langle S_z\rangle s_z$, where $\langle S_z\rangle=-(5/2)B_J[Sg\mu_B B/k_B(T+T_0)]$, with $B_J(x)$ as the Brillouin function, T_0 accounts for the reduced single-ion contribution due to the antiferromagnetic Mn-Mn coupling, and k_B is the Boltzmann constant. The parameters used in the calculation are chosen for $Ga_{1-x}Mn_xAs$, with $J_{sd}=N_0 j_{sd}x=-0.22x$ eV, where $N_0 j_{sd}$ is the exchange constant per cation for the material, $x=0.014$ is the Mn concentration, $g=-0.44$, $T_0=40$ K,[14,15] and $T=1$ K. For convenience we express all quantities in dimensionless units, using $\omega=eB_0/m^*$, and magnetic length $L_0=\sqrt{\hbar/eB_0}$. In this system $m^*=0.067m_e$, which results in $L_0=81$ nm and $\hbar\omega=0.17$ meV, for $B_0=0.1$ T as above.

The two-dimensional Schrödinger equation $H\Psi=E\Psi$ has solutions of the form $\Psi(x,y)=e^{iqy}\psi(x)$, where E is the total energy of the electron and q is the electron wave vector in the y direction. $\psi(x)$ satisfies

$$\left\{\frac{d^2}{dx^2}-V_e(x,\sigma_z)+\alpha_z^*\left[\sigma_x[q+A(x)]-\sigma_y\left(-i\frac{d}{dx}\right)\right]\right\}\psi(x) = -2E\psi(x), \tag{3}$$

$$V_e(x,\sigma_z)=[q+A(x)]^2+[J_{sd}^*\langle S_z\rangle+g^*B(x)]\sigma_z, \tag{4}$$

where $\alpha_z^*=2\alpha_z/(L_0\hbar\omega)$, $J_{sd}^*=2J_{sd}/\hbar\omega$, $g^*=g\mu_B B_0/\hbar\omega$, and V_e is the effective dynamical potential. We use the Landau gauge, $\vec{A}(x)=[0,A(x),0]$, and $B(x)=dA(x)/dx$. For the field configuration we treat here, the effective potential V_e results in an asymmetric double barrier structure (see bottom panel in Fig. 1) for different values of q. The bottom of the potential shifts differently for different spin values, and one of the barriers becomes larger as q increases so that the overall transmission is strongly suppressed for large q, as we will see below. The double barrier structure, as expected, gives rise to transmission resonances for small q, strongly affecting the transmission of the structure, as we will demonstrate.

For a magnetic barrier structure as that shown in Fig. 1, it is difficult to solve Eq. (3) analytically. However, a numerical approach which divides the region of the barrier $[x_i,x_f]$ into $N(\gg 1)$ segments of width $L=(x_f-x_i)/N$ is possible.[9] For small L (large N) the vector potential in each of the segments can be treated as constant so that in each jth segment one has solutions given by $\psi_j(x)_\pm=e^{ik_jx}\chi_\pm(k_j)$, with spinors

$$\chi_\pm(k_j)=\begin{pmatrix}\chi_\pm^1\\ \chi_\pm^2\end{pmatrix}, \tag{5}$$

where

$$\chi_\pm^1=\frac{-\alpha_z^*[q+A(x_j)+ik_j]}{\sqrt{2\lambda_\pm(\lambda_\pm-Z_j)}},$$

$$\chi_\pm^2=\frac{\lambda_\pm-Z_j}{\sqrt{2\lambda_\pm(\lambda_\pm-Z_j)}},$$

$$Z_j=J_{sd}^*\langle S_z\rangle+g^*B(x_j), \tag{6}$$

and

$$\lambda_\pm=\pm\{Z_j^2+|\alpha_z^*[q+A(x_j)+ik_j]|^2\}^{1/2}, \tag{7}$$

where k_j is the solution of the equation $\{k_j^2+[q+A(x_j)]^2-2E\}^2=\lambda_\pm^2$.

We consider the transmission of electrons with initial wave vectors $k^\uparrow$ and $k^\downarrow$ corresponding to the region $x\ll x_i$, which are the solutions of the problem with $J_{sd}\langle S_z\rangle=0$, and $\alpha_z=0$ away from the magnetic barrier region. It is clear that the transmission probabilities for electrons of spin eigenstates "↑" and "↓" are different due to the SOI, as well as due to the enhanced and inhomogeneous Zeeman splitting in Eq. (2). Since the wave vector in the y direction is fixed, on both incident and outgoing regions of the magnetic barrier, the wave function for spin-up incident electrons can be written as

$$\psi(x) = e^{ik^{\uparrow}x}\chi_{\uparrow} + r^{\uparrow\uparrow}e^{-ik^{\uparrow}x}\chi_{\uparrow} + r^{\downarrow\uparrow}e^{-ik^{\downarrow}x}\chi_{\downarrow}, \quad \text{for } x < x_i,$$
$$= t^{\uparrow\uparrow}e^{ik^{\uparrow}x}\chi_{\uparrow} + t^{\downarrow\uparrow}e^{ik^{\downarrow}x}\chi_{\downarrow}, \quad \text{for } x > x_f. \tag{8}$$

Here $t^{\uparrow\uparrow,\downarrow\uparrow}$ and $r^{\uparrow\uparrow,\downarrow\uparrow}$ are the transmission and reflection coefficients for the incident spin-up state $\chi_{\uparrow}$. Taking into account the boundary conditions, which require that the wave function be continuous at the interfaces, a system of linear equations for all these four coefficients can be derived. We emphasize that we have utilized extend boundary conditions to consider the case of an x-dependent SOI,[16] as we will assume in the specific examples below that the magnetic strip is likewise used as a gate that changes α_z locally. Once $t^{\uparrow\uparrow,\downarrow\uparrow}$ and $r^{\uparrow\uparrow,\downarrow\uparrow}$ are known, it is straightforward to obtain the spin-dependent transmission coefficients $T_{ss'}(E,q)$, where s' (s) is the incident (outgoing) spin, with $s,s'=\uparrow$ or $\downarrow$. Note that for incident electrons with spin $s'=\uparrow$ there are two kinds of transmission coefficients, $T_{\uparrow\uparrow}$ and $T_{\downarrow\uparrow}$, as the SOI produces precession of the electron spin as it propagates. A similar effect occurs for incident electrons with spin $s'=\downarrow$, although the presence of the magnetic field breaks time-reversal invariance, which results in a spin-filtering effect, as we will see below.

In the ballistic regime the spin-dependent conductance can be calculated from the Landauer-Büttiker formula,[7]

$$G_{ss'}(T) = \int_0^{\infty} g_{ss'}(E)\left(-\frac{\partial f(E,T)}{\partial T}\right)dE, \tag{9}$$

where

$$g_{ss'}(T) = G_0 \int_{-\pi/2}^{\pi/2} T_{ss'}(E, \sqrt{2E}\sin(\theta))\cos(\theta)d\theta, \tag{10}$$

θ is the angle of incidence with respect to the x direction (see top panel of Fig. 1), $f(E,T)$ is the Fermi-Dirac distribution function, and $G_0 = e^2 m^* v_F L_y / h^2$, where L_y is the length of the structure in the y direction and $v_F = \hbar k_F / m^*$ is the Fermi velocity.

To evaluate the electron spin polarization effect in the tunneling process, we define the net conductance polarization as

$$P = \frac{G_{\uparrow\uparrow} + G_{\uparrow\downarrow} - G_{\downarrow\uparrow} - G_{\downarrow\downarrow}}{G_{\uparrow\uparrow} + G_{\uparrow\downarrow} + G_{\downarrow\uparrow} + G_{\downarrow\downarrow}}. \tag{11}$$

III. RESULTS AND DISCUSSION

In Fig. 2 we show typical transmission coefficients, as functions of incident energy and angle ($q=\sqrt{2E}\sin\theta$), for an incoming electron with spin $\uparrow$. The upper panel shows the transmission coefficient for collected electrons with the same polarization, $T_{\uparrow\uparrow}$, while the lower is for outgoing electrons with opposite spins, $T_{\downarrow\uparrow}$. Here we use a typical SOI strength, $\alpha_z = 0.35 \times 10^{-11}$ eV m,[17] which corresponds to $\alpha_z^* = 0.5$. Notice that for low incident energy and/or with a large incident angle θ the transmission coefficients are very small, as the effective barrier presented by the magnetic strip is quite large (see bottom panel of Fig. 1). At lower incident angle and higher energy, the transmission exhibits a series of resonances near normal incidence ($\theta \approx 0$), as the magnetic vector potential results in an effective scattering double barrier potential [$V_e \simeq A^2(x)$ in Eq. (4)] with concomitant resonances. A simple analysis of the effective potential for each spin species which approximates its shape by a harmonic well at low energy yields values for the resonance energies very close to those obtained from the full calculation, allowing one to anticipate the resonant structure of T_{ss} from the device dimensions and field parameters. The resonance structure is also clearly seen in the spin mixing results, $T_{\downarrow\uparrow}$, as well as in the corresponding spin $\downarrow$ incidence, $T_{\downarrow\downarrow}$ and $T_{\uparrow\downarrow}$ (not shown), although with some subtle differences due to the asymmetry introduced by the field.

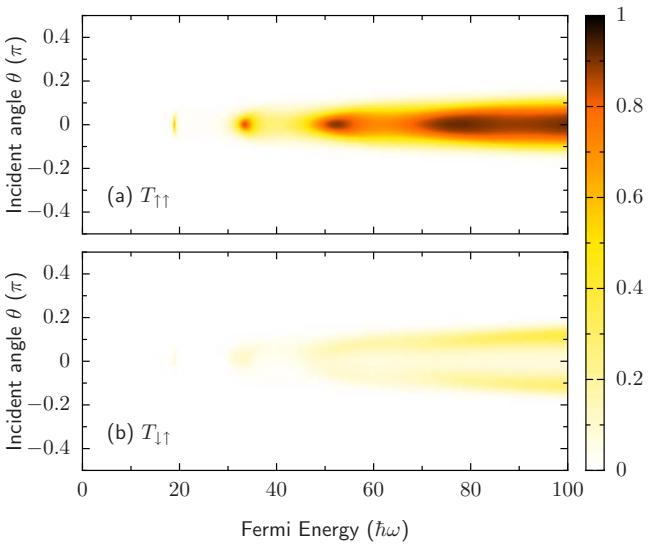

FIG. 2. (Color online) The transmission coefficients (a) $T_{\uparrow\uparrow}$ and (b) $T_{\downarrow\uparrow}$ as function of energy and incident angle θ for electrons tunneling through the magnetic barrier with perpendicular magnetization, $d=2L_0$, and SOI coupling $\alpha_z = 0.35 \times 10^{-11}$ eV m ($\alpha^* = 0.5$).

The calculated conductance and polarization components for the same parameters as in Fig. 2 are shown in Fig. 3, shown vs Fermi energy. The SOI naturally causes the spin of the electron to precess when the electron propagates through the gated region. This is evident in Fig. 3(a) as the spin-up conductance $G_{\uparrow\uparrow}$ is quite different from the spin-down conductance, $G_{\downarrow\downarrow}$. The inhomogeneous magnetic field also contributes significantly to change the tunneling probability of the electron through the magnetic gate barrier. $G_{\downarrow\downarrow}$ exhibits peaks shifted in general toward lower energy values, in contrast with those in $G_{\uparrow\uparrow}$, a behavior persisting at low energies, where the two curves show clearly split resonances.[18] In addition, the spin *mixing* probability of tunneling electrons depends only slightly on the incident spin for a given magnetic barrier, as illustrated by the curve for $G_{\uparrow\downarrow}$ being slightly different to $G_{\downarrow\uparrow}$ [see especially the inset in Fig. 3(a)].

The conductance polarization plotted in Fig. 3(b) shows that this structure results in polarization over 50% in the first resonant energy and close to 70% at the second and higher resonances. Therefore, for realistic values of strip magnetization and spin-obit coupling the system can generate substantial spin-polarized currents, *even as the injection is un-*

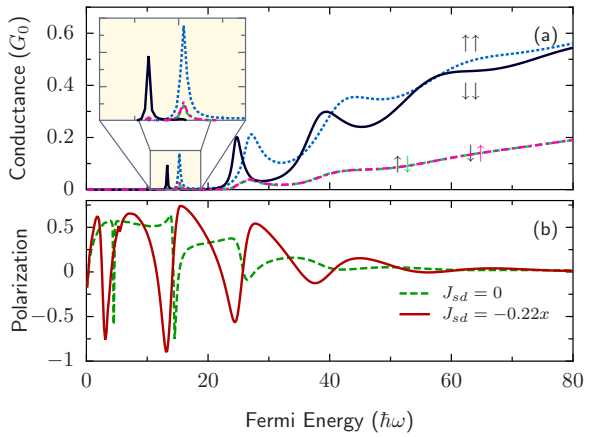

FIG. 3. (Color online) (a) Spin-dependent conductance (in units of G_0) and (b) polarization as function of Fermi energy (in units of $\hbar\omega$). Structure parameters as in Fig. 2. Panel (b) shows results for a nonmagnetic semiconductor system with J_{sd}=0 (dashed line). For x=0.014 here, nonzero J_{sd} is −3.1 meV.

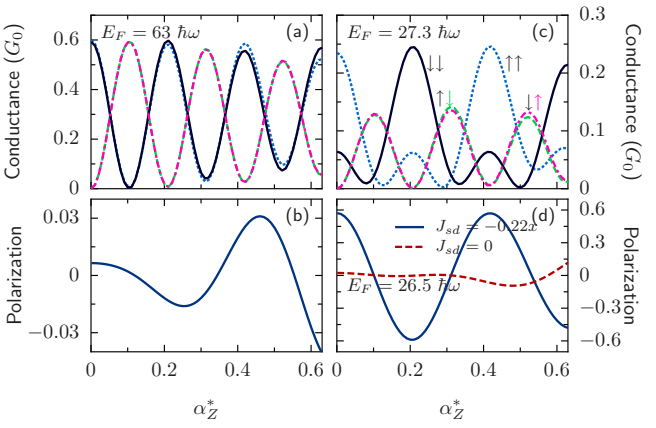

FIG. 4. (Color online) Spin conductance and polarization as function of α_z^* for different Fermi energies. Notice polarization exceeds 50% in panel (d) and reverses in a small α_z^* interval. Polarization is strongly suppressed in the absence of exchange, J_{sd}=0, even at the optimal resonance energy. Nonzero J_{sd} is −3.1 meV.

polarized. Notice that the resonant peaks created by the effective dynamic potential V_e are responsible for the large polarization values, as the latter decreases rapidly for higher Fermi energies.

Figure 3(b) also shows the resulting polarization whenever the exchange interaction is zero, J_{sd}=0 (dashed line), as it would be the case for the magnetic strip in a nonmagnetic semiconductor. We can see the same type of resonance-produced structure in the polarization since the nonvanishing g factor produces a (small) Zeeman splitting and correspondingly different V_e for the two spins. However, the presence of exchange greatly enhances the splitting of the resonances for the two spin species and produces a relatively slowly changing polarization with Fermi energy (or similarly with total magnetization value for a fixed energy). The slow variation in this dependence for DMS systems would in principle allow for more stable and better controlled spin polarization of the device.

To provide a more complete account of the role of SOI in this polarization effect we show in Fig. 4 the calculated conductance and polarization as functions of the SOI strength α_z^* at two different Fermi energies. Notice that α_z can be varied in experiments by the application of a gate voltage applied to the metallic strip itself, as we consider in our calculations. Figures 4(a) and 4(b) show results for E_F=63$\hbar\omega$. At this relatively large energy the spin-dependent conductances show regular oscillations with α_z^*, similar to those expected from the Datta-Das device.[5] In this region of SOI the polarization starts near zero (but nonvanishing, due to the Zeeman effect) and has a local maximum at α_z^*=0.45 of no larger than 3%, becoming slightly negative afterwards. Figures 4(c) and 4(d) show results for E_F=27.3$\hbar\omega$ near one of the transmission resonances in $G_{\downarrow\downarrow}$ in Fig. 3. It can be seen that increasing α_z^* results also in the spin conductances having oscillations. These features reflect the spin precession effects induced by the SOI, although further enhanced by the resonances of the dynamical potential, as discussed above. Notice that in this case, the conductance polarization can exceed 50% and be fully reversed when α_z^* changes by $\simeq$0.20. In comparison, panel (d) in this figure also shows the polarization for the same system but for J_{sd}=0 (dashed line), at the position of its corresponding resonance (E_F=26.5$\hbar\omega$). We see that the much smaller Zeeman splitting results in smaller amplitude oscillations of the polarization since the spin-up and spin-down resonances are much closer to each other and nearly cancel each other out.

As the strong spin polarization of the conductance is associated with the presence of transmission resonances through this combination of magnetic and electric-field barrier, we also explore its dependence on strip width—which determines the width of the effective double barrier potential V_e. In Fig. 5 we show the spin polarization vs Fermi energy for different magnitudes of the strip width d (d=L_0 to 4L_0). One can see that increasing d results in a larger width of the double barrier potential well produced by the effective potential, which in turn results in more resonant peaks in the conductance as the Fermi energy increases. In all cases, the polarization exceeds the 50% to 70% range. Notice also that the smoothness of the polarization transitions, as well as

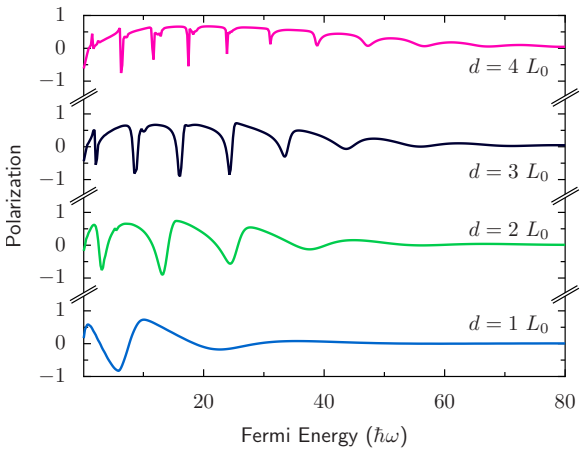

FIG. 5. (Color online) Spin polarization as function of Fermi energy at a given value of α_z^*=0.5 for several width values of the magnetic strip d. Curves offset for clarity.

their amplitude, is neither optimal for the first few resonances (too sharp) nor for the last few (too small polarization), but rather for the middle group. This would suggest the utilization of different Fermi energies for different strip widths, in order to maximize the spin polarization and its control. We should point out that the spin polarization due to magnetic strips reported earlier[11] is produced by quasibound states that appear preferentially for wider strips. The resonances we study here, however, appear even for narrow strips, as Fig. 5 shows.

In summary, we have shown that it is possible to achieve a substantial spin polarization in a realistic situation where a magnetized strip is placed in close proximity to a 2DEG. Our calculation incorporates the role of the giant Zeeman effect in diluted magnetic semiconductors, and this, together with the tunable SOI coupling, can be appropriately used to enhance or suppress the polarization in a controlled fashion. We should also notice that as the temperature changes, the effective field can be modulated, with the consequent changes on the spin polarization characteristics of a given structure.

ACKNOWLEDGMENTS

We thank D. Csontos and M. Zarea for helpful conversations. The authors are also thankful for the support of CMSS and BNNT programs at Ohio University, as well as NSF under Grants No. 0336431 and No. 0710581. J.V.B. acknowledges support of the A. von Humboldt Foundation.

[1] R. Winkler, *Spin-Orbit Coupling Effects in Two-Dimensional Electron and Hole Systems*, Springer Tracts in Modern Physics Vol. 191 (Springer, Berlin, 2003).

[2] S. A. Wolf, D. D. Awschalom, R. A. Buhrman, J. M. Daughton, S. von Molnar, M. L. Roukes, A. Y. Chtchelkanova, and D. M. Treger, Science **294**, 1488 (2001).

[3] I. Žutić, J. Fabian, and S. Das Sarma, Rev. Mod. Phys. **76**, 323 (2004).

[4] *Semiconductor Spintronics and Quantum Computation*, edited by D. D. Awschalom, D. Loss, and N. Samarth (Springer, Berlin, 2002).

[5] S. Datta and B. Das, Appl. Phys. Lett. **56**, 665 (1990).

[6] W. Yang, K. Chang, X. G. Xu, and H. Z. Zheng, Appl. Phys. Lett. **88**, 082107 (2006); W. Yang, K. Chang, X. G. Xu, H. Z. Zheng, and F. M. Peeters, *ibid.* **89**, 132112 (2006).

[7] A. Matulis, F. M. Peeters, and P. Vasilopoulos, Phys. Rev. Lett. **72**, 1518 (1994).

[8] P. D. Ye, D. Weiss, R. R. Gerhardts, M. Seeger, K. von Klitzing, K. Eberl, and H. Nickel, Phys. Rev. Lett. **74**, 3013 (1995); M. Cerchez, S. Hugger, T. Heinzel, and N. Schulz, Phys. Rev. B **75**, 035341 (2007).

[9] J. Q. You, L. Zhang, and P. K. Ghosh, Phys. Rev. B **52**, 17243 (1995).

[10] M.-W. Lu, L.-D. Zhang, and X.-H. Yan, Phys. Rev. B **66**, 224412 (2002); Y. Jiang and M. B. A. Jalil, J. Phys.: Condens. Matter **15**, L31 (2003); F. Zhai and H. Q. Xu, Appl. Phys. Lett. **88**, 032502 (2006).

[11] F. Zhai and H. Q. Xu, Phys. Rev. B **72**, 085314 (2005); Phys. Rev. Lett. **94**, 246601 (2005).

[12] A. Lemaitre, C. Testelin, C. Rigaux, T. Wojtowicz, and G. Karczewski, Phys. Rev. B **62**, 5059 (2000).

[13] J. C. Egues, Phys. Rev. Lett. **80**, 4578 (1998).

[14] R. Lang, A. Winter, H. Pascher, H. Krenn, X. Liu, and J. K. Furdyna, Phys. Rev. B **72**, 024430 (2005).

[15] N. Dai, L. R. Ram-Mohan, H. Luo, G. L. Yang, F. C. Zhang, M. Dobrowolska, and J. K. Furdyna, Phys. Rev. B **50**, 18153 (1994).

[16] U. Zülicke and C. Schroll, Phys. Rev. Lett. **88**, 029701 (2001); L. Zhang, P. Brusheim, and H. Q. Xu, Phys. Rev. B **72**, 045347 (2005).

[17] C. F. Destefani, S. E. Ulloa, and G. E. Marques, Phys. Rev. B **70**, 205315 (2004).

[18] Notice that the transmission resonance peak that is shifted to lower energies (here the down spin) depends predominantly on the polarization of the magnetic impurities. For the system studied here, the spin-down state is lower in energy, as experimentally determined in Ref. 14.